

The WAAS L5 Signal

An Assessment of Its Behavior and Potential End Use

Hyunho Rho and Richard B. Langley

THE RECENT LAUNCH of the GPS Block IIR-20(M) satellite and the commissioning of its L5 demonstration payload herald the beginning of a bright new era in space-based positioning, navigation, and timing. The new satellite signal is anticipated to provide better-quality range measurements and possibly improve the tracking performance of a GPS receiver compared with current civil L1 and L2 signals through use of improved signal structures. The L5 signal will be standard on the future Block IIF and Block III satellites.

However, some readers may be surprised to learn that L5 signals have been continuously transmitted by a pair of satellites for the past several years. The geostationary Earth-orbiting (GEO) satellites used by the U.S. Federal Aviation Administration's (FAA's) Wide Area Augmentation System to provide enhanced integrity and accuracy include not only an L1 payload but an L5 payload as well. While the WAAS L5 signals have been broadcast from space for some time, they did not come from a satellite in medium Earth orbit, and so it was necessary to include the demonstration payload on the GPS Block IIR-20(M) satellite to guarantee the L5 frequency filing with the International Telecommunication Union.

There are some differences between the WAAS L5 signals and the future fully fledged GPS L5 signals. The WAAS L5 signals only use a single-channel carrier (there is no quadrature or Q channel) and the data rate is 250 bits per second (bps) rather than 50 bps. The WAAS signals are actually generated on the ground and relayed through the GEOs using a "bent pipe" approach. The FAA uses the L5 signals, in conjunction with the L1 signals, to compute ionospheric delays as part of the closed-loop control of the broadcast signals.

Although the WAAS L5 signals are not yet intended for end users, can they be used now for positioning and navigation and, if so, are there any caveats? In this month's column, I am joined by one of my graduate students, Hyunho Rho, who has looked at the WAAS L5 transmissions, examining their signal strengths, multipath characteristics, and instrumental bias issues. Precise positioning performance of WAAS pseudoranges has also been assessed as an independent check on instrumental bias compensation by the WAAS control segment. The favorable results point to a future of the L5 signal, on both the WAAS satellites and the next-generation GPS satellites, which is bright indeed.

"Innovation" is a regular column that features discussions about recent advances in GPS technology and its applications as well as the fundamentals of GPS positioning. The column is coordinated by Richard Langley of the Department of Geodesy and Geomatics Engineering at the University of New Brunswick, who welcomes your comments and topic ideas. To contact him, see the "Contributing Editors" section on page 6.

As part of the GPS modernization effort, a new third civil signal, L5 at 1176.45 MHz, will join the current civil legacy signal on L1 at 1575.42 MHz and the second civil signal on L2 (L2C) at 1227.60 MHz, which is also being deployed during the modernization effort. This new satellite signal is anticipated to provide better quality range measurements and possibly improve the tracking performance of a GPS receiver compared with the current L1 and L2 signals by adopting improved signal structures.

This includes increasing the chipping rate to 10.23 megachips per second (Mcps) compared to 1.023 Mcps for the L1 C/A (C1) code, a longer spreading code than L1 C1, and a higher transmitted power than that of the L1/L2 signals (see **TABLES 1** and **2**). It will also be beneficial for mitigating the ionospheric error — potentially the largest GPS error source for most civil users — by use of the multiple frequencies. More detailed descriptions of the L5 signal can be found in publications listed in Further Reading.

Since the Wide Area Augmentation System (WAAS) should be compatible with GPS modernization, both of the current WAAS geostationary Earth-orbiting satellites (GEOs), Intelsat's Galaxy XV (PRN135) and TeleSat's Anik F1R (PRN138), contain L1 and L5 WAAS payloads and broadcast both signals on the air. The WAAS payloads are operated by Lockheed Martin for the Federal Aviation Administration.

The WAAS L5 signal structure is similar to the GPS L5 signal except that only a single channel carrier is used, and the data rate is increased to 250 bits per second (bps). The different characteristics of the GPS and WAAS signals are illustrated in Table 1.

A receiver equipped with specialized



INNOVATION INSIGHTS
with Richard Langley

L5 signals have been continuously transmitted by a pair of satellites for the past several years.

	GPS L5	WAAS L5	GPS/WAAS L1
Carrier Frequency	1176.45 MHz	1176.45 MHz	1575.42 MHz
Signal Structure	Two carrier components: I5 and Q5 ranging codes	Single carrier component: C5 ranging code	Two carrier components: P(Y) and CA/CA ranging code (WAAS)
Code Length (chips)	10230	10230	1023
Code Rate	10.23 Mcps	10.23 Mcps	1.023 Mcps
Data Rate	50 bps	250 bps	50/250 bps

▲ **TABLE 1** Characteristics of GPS L5 signal vs. WAAS L5

firmware that allows acquisition of both L1 and L5 signals simultaneously from the WAAS GEOs was used to obtain test data sets at the University of New Brunswick (UNB) in Fredericton, Canada. A data set spanning four continuous days in August 2008 has been used to study the WAAS L5 signals.

This article discusses the overall observation quality of the WAAS L5 signal. Since the carrier-power-to-noise-density ratio (C/N_0) indicates the level of signal power versus the level of background noise in the observables, C/N_0 was used as a first signal quality indicator, and the C/N_0 values of the L1 and L5 signals were compared. The receiver tracking noise and multipath (MP) characteristics of the L1 and L5 signals were also compared. In this comparison, the magnitude of the possible improvement from the enhanced signal structures in the L5 signal is quantified.

In the following sections, the WAAS differential code bias (DCB) between L1 C1 and L5 code (C5) are analyzed. Since the WAAS GEO ranging signals are generated by the ground control segment and uplinked to the GEO satellites for rebroadcast, the ionospheric delays as well as the DCBs should be estimated and compensated for in both the uplink and downlink signals. Since another important role of DCBs in WAAS might be to resolve the clock referencing issue in the observables for single-frequency users (like the group delay term, T_{GD} , for GPS L1/L2),

SV Blocks	Channel	Signal	
		P(Y)	C/A or L2C
II/IIA/IIR	L1	-161.5 dBW	-158.5 dBW
	L2	-164.5 dBW	N/A
IIR-M/IIF	L1	-161.5 dBW	-158.5 dBW
	L2	-161.5 dBW	-160.0 dBW
IIF	L5	I5	Q5
		-157.9 dBW	-157.9 dBW

▲ **TABLE 2** Received minimal signal strength

SV	Signal	Min.	Max.	Mean	Std. Dev.
PRN138	L1	46.60	48.00	47.35	0.19
	L5	46.30	47.60	46.86	0.21
PRN135	L1	40.80	44.30	42.85	0.48
	L5	41.50	44.30	42.93	0.41

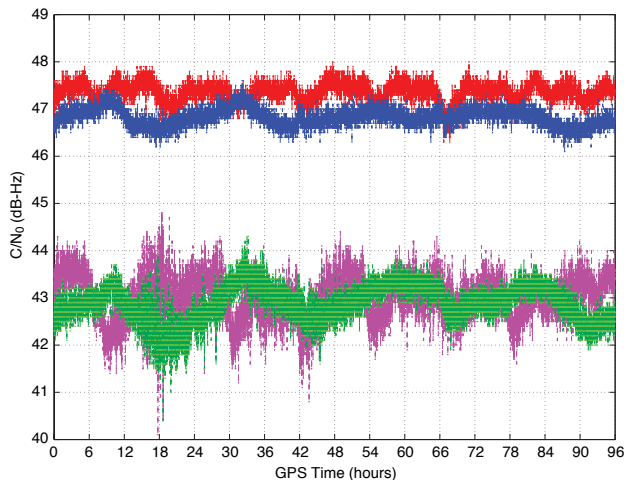
▲ **TABLE 3** Statistics of the observed C/N_0 values for the WAAS GEOs, PRN135 and PRN138, for a four-day continuous period. (Units: dB-Hz)

the overall behavior of the estimated DCBs were further analyzed. Finally, the possible benefit of using WAAS GEO ranging measurements in the positioning domain is also discussed.

Observability of L5 Signals at UNB

WAAS currently transmits both L1 and L5 signals on the air. At UNB, the two WAAS GEOs, PRN135 and PRN138, can be simultaneously monitored. Both GEOs are visible to the southwest with PRN135 at an elevation angle of 7.6° and azimuth of 252.6° , while PRN138 is at an elevation angle of 23.9° and azimuth of 230.1° .

To obtain test data sets at UNB, we used a receiver equipped with specialized firmware that allows acquisition of both L1 and L5 signals simultaneously from the WAAS GEOs. The first four



▲ **FIGURE 1** Carrier-power-to-noise-density ratio (C/N_0). The magenta and green dots represent the PRN135 C/N_0 values for L1 and L5, respectively. The red and blue dots represent the PRN 138 C/N_0 values for L1 and L5, respectively.

channels of the entire 32-channel-configured receiver were assigned to the two WAAS GEOs for L1 and L5 dual-frequency tracking and the other 28 channels were used for general GPS L1 and L2 dual-frequency tracking. With this capability, the observation quality of the WAAS L5 signals could be directly compared with the WAAS L1 signals, and the simultaneous GPS dual-frequency measurements could be used for other purposes such as comparing the differences of the estimated DCBs for GPS and for WAAS.

Because PRN135 is seen at the low elevation angle of 7.6° , an elevation cutoff angle of 0° was used to collect data from all satellites. The collected data set for the continuous four days of August 24–27, 2008, has been used to assess the quality of the L1 C1 and L5 C5 code measurements (pseudoranges).

Test Results and Analyses

In this section, we investigate the overall quality of the WAAS L5 signal by comparing the C/N_0 values provided directly by the receiver. The computed MP1 and MP5 observables are also compared. We then discuss the characteristics of the WAAS GEO satellite DCBs and the possible benefit of using WAAS GEO ranging measurements in the positioning domain.

Carrier-Power-to-Noise-Density Ratio. According to the official signal specifications, the transmitted signal power of the GPS L5 signal should be 0.6 dBW higher than that of the L1 C1 signal (see also Table 2).

To see the differences in the transmitted power of the actual WAAS L5 signal versus the L1 signal, the observed C/N_0 values of the L1 and L5 signals from both GEOs, PRN135 and PRN138, are illustrated in **FIGURE 1**.

In the figure, we can first see that the overall C/N_0 values for the L1 and L5 signals from both GEOs, vary in time in the range of about ± 1 dB-Hz. Those variations might be explained by atmospheric effects or actual transmitted power fluctuations.

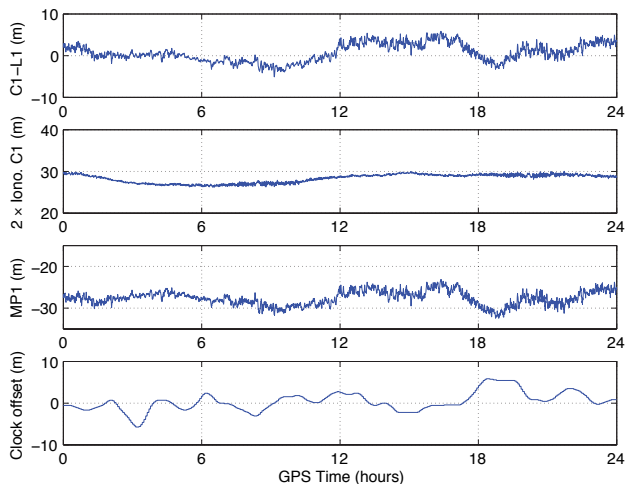
By comparing the C/N_0 values between PRN138 and PRN135, we can also see that the C/N_0 values have clear elevation angle dependence. Also the C/N_0 values from the higher elevation angle GEO, PRN138, have smaller variations in time than those of PRN135.

The results illustrated in Figure 1 show that the observed WAAS L5 C/N_0 values are comparable with the L1 C/N_0 values for both GEOs. The compiled statistics of the observed C/N_0 values shown in **TABLE 3** also show that the C/N_0 values of the L1 and L5 signals are comparable with the used equipment.

Code Multipath and Noise Level Analysis. In this sub-section, the multipath and noise level (MP) of C1 and C5 codes for both WAAS GEOs are analyzed. The MP observables referred to frequencies L1 and L5 were computed by combining code and carrier-phase observations in the usual way. See “Evaluation of the New WAAS L5 Signal” in Further Reading for details.

To see a detailed view of each step of the computations, the step-by-step results are illustrated in **FIGURES 2** and **3**. These figures show single-day results of the computed MP1 and MP5 values for PRN138 on August 25, 2008. In the top panels, the C1-L1 observable and C5-L5 observable, which contain twice the ionospheric delays, ambiguity, satellite and receiver differential code bias, and combined carrier-phase and pseudorange MP values, are illustrated. The compared results show that the noise level of the C1-L1 observable is higher than that of C5-L5 observable.

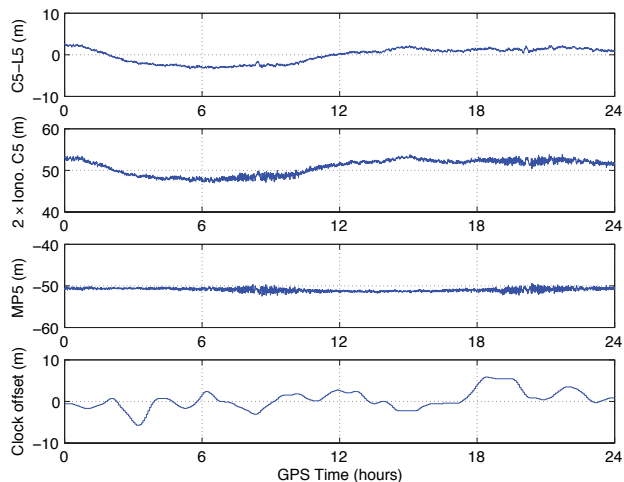
By comparing the second and third panels in Figure 3, we can see that the twice-ionospheric-delay terms which are properly scaled to each observable C1 and C5 could be the main source of the low frequency time variations in the C5-L5 observable. After removing the ionospheric term, the remaining terms are only the constant ambiguity and slowly varying hardware delays. Therefore, the MP5 observable is more or less like a constant (plus noise), even though there exists a certain amount of bias that is caused by the carrier-phase ambiguities.



▲ **FIGURE 2** MP1 and related quantities for PRN138 on August 25, 2008. The y-axis range of all subplots is fixed at 20 meters.

However, the MP1 observable in the third panel of Figure 2 shows different characteristics compared to the MP5 observable. The characteristics of the MP1 observable could be described as a constant bias that is caused by the ambiguity and MP effect, and a variable pattern of unknown origin at the moment. If the carrier-phase ambiguities and the satellite and receiver DCB can be assumed as constant terms, the MP1 observable should behave like the MP5 observable. To see if there exists any correlation between the computed MP values and the GEO satellite clock offset, which is provided by the WAAS GEO navigation message, correlation coefficients between the MP observables and the GEO satellite clock offsets were computed. The results show that the correlation coefficient between MP1 and GEO clock offset was -0.360 and it was -0.110 for the MP5. Those results show that there is a minor degree of correlation, if any.

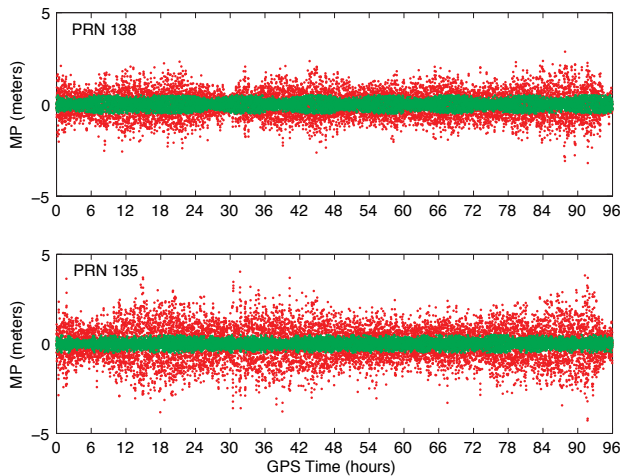
To see if the time-varying term in the MP1 observable is only observed on a specific day and if it also happened for the other GEO, PRN135, the MP1 and MP5 observables from both GEOs were computed for a continuous four-day sample. The results show that the MP1 observables from both GEOs contain a time-varying term that is not seen in the MP5 observables for the four continuous sample days. However, the time-varying term in the MP1 observables have been identified as a contribution of the satellite DCB between C1 and C5 as discussed in the



▲ **FIGURE 3** MP5 and related quantities for PRN138 on August 25, 2008. The y-axis range of all subplots is fixed at 20 meters.

following section.

Since one of our purposes in this section is to see the overall performance of the new L5 C5 code compared to the L1 C1 code in terms of the noise level, a moving average filter was adopted to compute the final MP values in which the high frequency noise is reduced. For the computation, cycle-slips in the carrier-phase measurements were identified first and the moving average filter



▲ **FIGURE 4** Difference between original and moving-average-filtered values for MP1 (red dots) and MP5 (green dots) for PRN135 and PRN138 for August 24–27, 2008

applied to each separate arc with a window size of 10 measurements for both L1 C1 and L5 C5 code measurements.

FIGURE 4 shows the time series of the moving average filtered MP values for L1 C1 and L5 C5 codes for both GEOs. In the figure, we can clearly see that the MP5 values have a better quality in terms of noise level compared with MP1 values. This is explained by the enhanced signal structure of the L5 signals. The L5 C5 code has a higher chipping rate of 10.23 Mcps than the L1 C1 code of 1.023 Mcps, making the main peak in the cross-correlation function sharper by a factor of ten, and improving noise performance and mitigating multipath effects.

Satellite and Receiver Differential Code Bias. The ionospheric delays as well as satellite and receiver DCBs should be estimated and compensated for when generating the two signals, L1 and L5, which are uplinked to the GEOs.

To identify the overall behavior of DCBs in the GPS satellites and WAAS GEOs, we first generated the DCB observables for GPS PRN10 on August 25, 2008. For GPS, we used L1 C1 and L2 P2 measurements to generate DCB observables.

However, note in this section that we also use the same term, DCB, to represent the differential carrier-phase bias for simplicity.

FIGURE 5 shows the computed combined satellite and receiver DCB for the pseudorange measurements and the carrier-phase measurements for GPS PRN10. Since PRN10 had few cycle slips on this day, with a long unbroken arc with the elevation angle ranging from about 10° to 85°, this satellite was chosen to illustrate the effect of DCB on GPS observations.

In the second panel, the observed slant ionospheric delays using pseudoranges are much noisier than those of carrier-phase measurements. The panel also shows that the noise level of the ionospheric measurements is elevation-angle dependent as we expect. However, the overall variations of the observed pseudorange ionospheric delays in time are the same as those of the carrier-phase ionospheric measurements except for a residual bias,

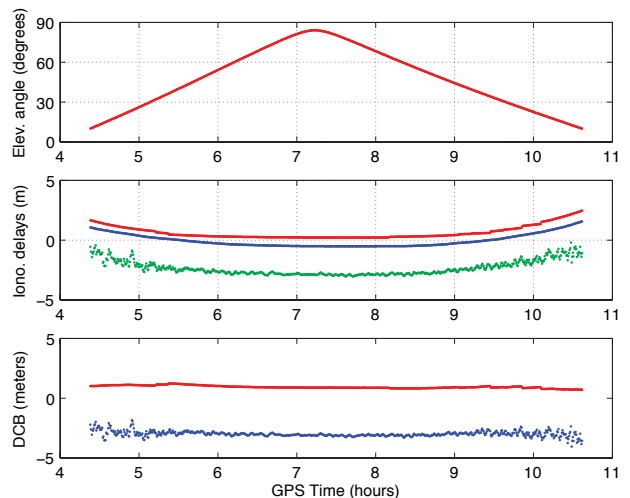
which is caused by not fully accounting for the ambiguity in the carrier-phase measurements.

Since we used the WAAS ionospheric corrections as a reference to generate the DCB observables, the different DCBs for carrier-phase and pseudorange ionospheric measurements in the third panel could be generated. And the differences between carrier-phase DCB and pseudorange DCB in the third panel could be explained by the residual carrier-phase ambiguity as well as a difference in the hardware delay bias between carrier-phase and pseudorange observables. However, with this approach, it should be noted that the accuracy of the computed DCBs are dependent on the accuracy of the WAAS ionospheric corrections. The user ionospheric range errors for the WAAS ionospheric delay corrections varied from 0.3 to 2.9 meters for this satellite. With that accuracy, it might not be enough to precisely determine the different hardware delay biases between pseudorange and carrier-phase observables.

However, both computed DCBs using pseudorange and carrier phase do not vary significantly in time, indicating that the combined satellite and receiver bias is almost constant.

To take advantage of the precise but ambiguous carrier-phase ionospheric observables versus the unambiguous but less precise pseudorange ionospheric observables, we used the carrier-phase leveling technique.

In **FIGURE 6**, the top panel shows the elevation angle change over a day for PRN138. It shows that even though PRN138 is a geostationary satellite, there is some degree of movement. In the second panel, the leveled ionospheric delays could be identified



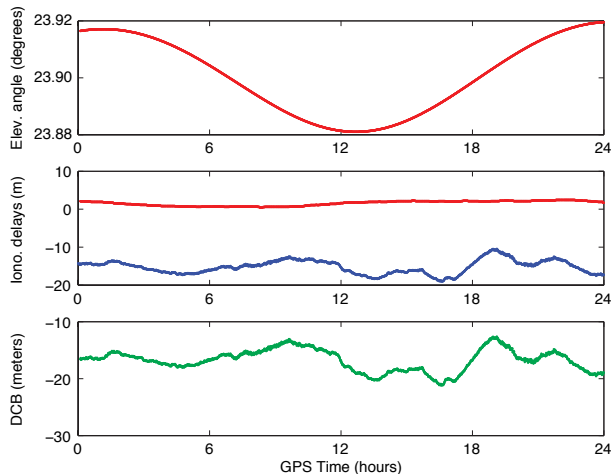
▲ **FIGURE 5** Computed satellite and receiver combined DCB for GPS PRN10 on August 25, 2008. The red dots in the second panel show the computed relative ionospheric delays by using L1 and L2 carrier-phase measurements, the blue dots represent the ionospheric delays computed by using WAAS ionospheric corrections, and the green dots show the computed ionospheric delays using C1 and P2 pseudorange measurements. The red dots in the third panel show computed carrier-phase DCB and the blue dots show the computed pseudorange DCB.

as having more variation in time than the ionospheric delays computed from the WAAS corrections. And, finally, the differences between leveled ionospheric delays and WAAS ionospheric delays were computed as DCB estimates and illustrated in the third panel.

To see if there is any correlation between estimated DCB values and the time variations that we observed in the WAAS MP1 observable, we conducted a correlation analysis.

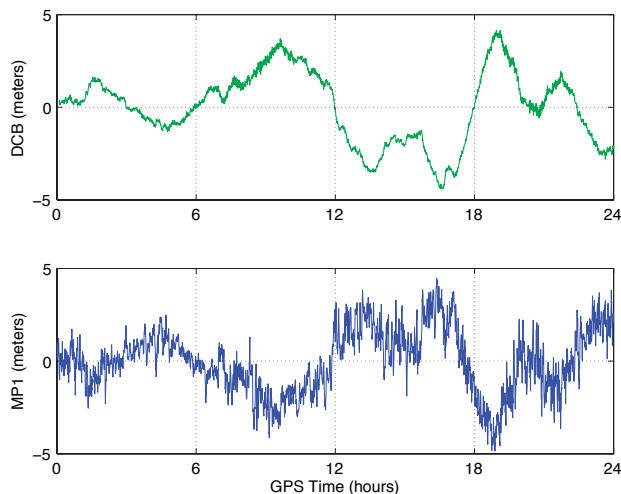
Since the receiver DCB is common for all monitored satellites and observed to be more or less constant in time, as we saw in Figure 5, we took a mean of computed DCBs for all satellites and subtracted that value from the computed DCBs. In this case, the remaining term represents the variation of the satellite DCB versus the constant mean, which is illustrated in the first panel of **FIGURE 7**. To compare the overall correlation between the estimated DCB and MP1 at the same level, the mean bias of all the MP1 values was also removed and is illustrated in the second panel of Figure 7.

Finally, we can see that there is a strong anti-correlation between the variations of satellite DCB and the MP1 value. The correlation coefficient between the satellite DCB and the MP1 values was -0.856. WAAS currently does not provide the C1-C5 DCB value in the transmitted WAAS messages. However, if the WAAS satellites operated in the same way as GPS satellites, single frequency



▲ **FIGURE 6** Computed satellite and receiver combined DCB for WAAS PRN 138 on August 25, 2008. In the second panel, the red dots show the computed ionospheric delays using WAAS ionospheric corrections and the blue dots represent the carrier-phase-leveled ionospheric delays.

WAAS GEO ranging users would need the DCB value to resolve the clock referencing issue to use single-frequency code observations for positioning. To circumvent this issue, it appears WAAS compensates for the C1-C5 bias in producing the L1 signal at the control segment. In this way, the single-frequency WAAS GEO



▲ **FIGURE 7** Correlation between estimated DCB and WAAS MP1 for PRN138

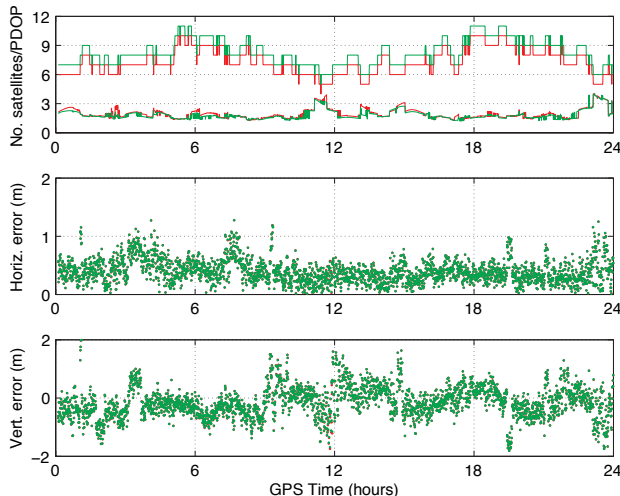
ranging user does not need to consider the satellite DCB term.

Positioning Domain Results. To see if the C1-C5 satellite DCBs have been compensated for in producing the WAAS GEO L1 C1 signals, the residuals from position-determination software of the C1 code measurements for PRN138 have been analyzed. To process GPS plus PRN138 L1 C1 pseudoranges, the UNB wide-area differential GPS point positioning software has been used.

In processing the data, we applied the GPS satellite orbit and clock corrections provided in the WAAS messages. WAAS does not provide the orbit and clock corrections for the GEOs, above and beyond the GEO orbit and clock data in WAAS messages. WAAS-provided ionosphere delay corrections have been applied for both GPS satellites and PRN138. The UNB3 tropospheric delay model including Niell mapping functions was used to mitigate the troposphere errors for both GPS satellites and PRN138.

To account for receiver noise and multipath, an elevation-angle-dependent empirical stochastic model was used. However, since the residual GPS orbit and clock errors (less than 1 meter) and the WAAS GEO orbit and clock errors (more than 10 meters based on the GEO user range error [URA]) are different, different weighting schemes have been applied to the GPS and WAAS data. For the GPS satellites, the initial GPS orbit error was set to a conservative 3 meters even though, after WAAS orbit corrections for the GPS satellites are applied, residual errors are less than 1 meter. The GEO satellite accuracy of 10 meters was determined based on the URA provided by the WAAS GEO navigation message and also from analyzing the positioning results. In most cases, the URA index of the WAAS GEO satellites was 6, which indicated that the accuracy of GEO orbits was in the range of 13.65 to 24.0 meters, making the 10-meter value used for the positioning process slightly optimistic.

In **FIGURE 8**, the overall improvement of the positioning results by using the WAAS GEO satellite is seen to be negligible. The 95th percentile horizontal error was 0.783 meters and the 95th



▲ **FIGURE 8** Benefit of using WAAS GEO ranging in point positioning. The top panel shows the number of satellites that have been used for the point positioning process and PDOP and the lower panels show the positioning results. The green traces and points show the results of using GEO ranging data and the red traces and points show the results without using WAAS GEO ranging measurements.

percentile vertical error was 1.091 meters when only the GPS measurements were used. When the WAAS GEO PRN138 ranging measurements were added, the result was the same for the 95th percentile horizontal error and 1.087 meters for the 95th percentile vertical error.

Those negligible effects on the positioning results by adding WAAS GEO ranging to the GPS measurements might be explained by the weighting scheme that we used. Because of the low elevation angle of the PRN138 measurements with relatively less accurate GEO orbits than GPS, the weight of the GEO measurements was set to be much less than that of the GPS measurements. Therefore, the contributions of the WAAS GEO ranging measurements were not significant compared with the GPS measurements in the point positioning process for the particular data set used with a large number of GPS satellites observed.

However, as the first panel in Figure 8 shows, the benefit of using the WAAS GEO ranging measurements in the point positioning process is in the improvement of dilution of precision (DOP) values. So it might be more beneficial to use WAAS GEO ranging measurements in more challenging situations where the number of monitored GPS satellites is quickly changing, and where fewer satellites are monitored such as in a kinematic scenario. Likely in such situations, there will be better positioning results if both WAAS GEOs are used for positioning as well as GPS satellites.

Conclusions

The WAAS L5 signal has been evaluated by comparing selected signal quality indices for the L1 and L5 signals. C/N_0 values for the WAAS GEOs, PRN135 and PRN138, were compared on the L1 and L5 frequencies. The result showed that the strength

of the WAAS L5 signal is similar to that of the C1 code on the L1 frequency (within ± 1 dB-Hz) with our receiver and antenna setup.

By comparing the multipath-plus-noise level of the L1 C1 and L5 C5 code data, we found that the enhanced signal structure of L5 has a better quality in terms of multipath-plus-noise level compared to the L1 C1 code.

Currently, the WAAS control segment is using dual-frequency data from the GEOs. By examining the multipath-plus-noise and estimated DCB values, we found that WAAS GEO satellite DCBs appear to vary in time and that the WAAS control segment compensates for the C1-C5 DCB bias when producing the L1 C1 signal.

The positioning domain results indicate that a proper weighting scheme should be used for combining WAAS GEO range measurements with GPS measurements.

Finally, it should be pointed out that although WAAS transmits L5 signals, the signals are not intended for end users at this time and should be used with caution.

Acknowledgments

The research reported in this article was supported by the Natural Sciences and Engineering Research Council of Canada. The authors thank NovAtel Inc. for supplying the receiver used in this research as well as the special firmware used. This article is based on the paper "Evaluation of the New WAAS L5 Signal" presented at ION GNSS 2008, the 21st International Technical Meeting of the Satellite Division of The Institute of Navigation, held in Savannah, Georgia, September 16–19, 2008.

HYUNHO RHO received an M.Sc. in 1999 in geomatics from Inha University, South Korea. He is a Ph.D. candidate in the Department of Geodesy and Geomatics Engineering at the University of New Brunswick, where he is investigating ways to improve ionospheric modeling for wide area differential GPS (WADGPS) and precise point positioning with WADGPS corrections.

Manufacturers

A **NovAtel** (www.novatel.com) ProPak-V3 (OEM-V3) receiver was used with a **Trimble** (www.trimble.com) Zephyr Geodetic 2 antenna. 

FURTHER READING

■ Authors' Proceedings Paper

"Evaluation of the New WAAS L5 Signal" by H. Rho and R.B. Langley in *Proceedings of ION GNSS 2008*, the 21st International Technical Meeting of the Satellite Division of The Institute of Navigation, Savannah, Georgia, September 16–19, 2008, pp. 1667–1678.

■ Signal Specifications

Interface Specification, IS-GPS-200, Revision D (IRN-200D-001), Navstar GPS Space Segment/Navigation User Interfaces, ARINC Engineering Services, LLC, El Segundo, California, March 7, 2006.

Interface Specification, IS-GPS-705 (IRN-705-003), Navstar GPS Space Segment/User Segment L5 Interfaces, ARINC Engineering Services, LLC, El Segundo, California, September 22, 2005.

"The New L5 Civil GPS Signal" by A.J. Van Dierendonck and C. Hegarty in *GPS World*, Vol. 11, No.9, September 2000, pp. 64–72.

Minimum Operational Performance Standards for Global Positioning System/Wide Area Augmentation System Airborne Equipment (WAAS MOPS), RTCA/DO-229D, RTCA Inc., Washington, D.C., December 13, 2006.

■ Wide Area Augmentation System Improvements

"Good, Better, Best: Expanding the Wide Area Augmentation System" by T.R. Schempp in *GPS World*, Vol. 19, Issue 1, January 2008, pp. 62–67.

■ Wide Area Augmentation System Biases

"What are WAAS GEOs' L1 and L5 Differential Biases and How Are

They Estimated?" by M.S. Grewal in *GNSS Solutions, Inside GNSS*, Vol. 3, No. 4, May/June 2008, pp. 18–23.

"Method and Apparatus for Wide Area Augmentation System Having L1/L5 Bias Estimation" by P.-H. Hsu, L. Cheung, and M. Grewal, United States Patent 20070067073, Publication Date March 22, 2007.

"Prototype Test Results of L1/L5 Signals of Future GEO Satellites" by P.-H. Hsu, L. Cheung, and M. Grewal in *Proceedings of ION GNSS 2004*, the 17th International Technical Meeting of the Satellite Division of The Institute of Navigation, Long Beach, California, September 21–24, 2004, pp. 1359–1366.

■ Precise Point Positioning with Wide Area Corrections

"Dual-frequency GPS Precise Point Positioning with WADGPS Corrections" by H. Rho and R.B. Langley in *Proceedings of ION GNSS 2005*, the 18th International Technical Meeting of the Satellite Division of The Institute of Navigation, Long Beach, California, September 13–16, 2005, pp. 1470–1482.

■ Positioning Using Satellite-Based Augmentation System Data

"The Future is Now: GPS + GLONASS + SBAS = GNSS" by L. Wanninger in *GPS World*, Vol. 19, No. 7, July 2008, pp. 42–48.

■ Ionospheric Effects and Modeling

Global Ionospheric Total Electron Content Mapping Using the Global Positioning System by A. Komjathy, Ph.D. dissertation, Department of Geodesy and Geomatics Engineering Technical Report No. 188, University of New Brunswick, Fredericton, Canada, September 1997.

COPYRIGHT 2009 QUESTEX MEDIA GROUP, INC. All rights reserved. No part of this publication may be reproduced or transmitted in any form or by any means, electronic or mechanical including by photocopy, recording, or information storage and retrieval without permission in writing from the publisher, Questex Media Group, Inc. Authorization to photocopy items for internal/educational or personal use, or the internal/educational or personal use of specific clients is granted by Questex Media Group, Inc. for libraries and other users registered with the Copyright Clearance Center, 222 Rosewood Dr., Danvers, MA 01923, 978-750-8400 fax 978-750-4470. For uses beyond those listed above, please direct your written request to questexpersmissions@reprintbuyer.com or 800-494-9051, Ext. 100.

PRIVACY NOTICE: Questex Media Group provides certain customer contact data (such as customers' names, addresses, phone numbers and e-mail addresses) to third parties who wish to promote relevant products, services and other opportunities which may be of interest to you. If you do not want Questex Media Group to make your contact information available to third parties for marketing purposes, simply call toll-free 866-344-1315 or 1-847-763-9594 (Outside the US) between the hours of 8:30 am and 5 pm (CT) and a customer service representative will assist to remove your name from Questex's lists.

GPS WORLD (ISSN 1048-5104) is published monthly (12 issues/yr) by Questex Media Group, Inc., 306 W Michigan St, Ste 200, Duluth, MN 55802. **SUBSCRIPTION RATES:** U.S. and possessions — 1 year (12 issues), \$67; 2 years (24 issues), \$117. Canada and Mexico — \$87, 1 year; \$137, 2 years. All other countries — \$127, 1 year; \$232, 2 years. International pricing includes air-expedited service. Single copies (prepaid only): \$7 in the United States, \$9 all other countries. Back issues, if available, are \$19 in the U.S. and possessions, \$23 all other countries. Include \$6.50 per order plus \$2 per additional copy for U.S. postage and handling. Periodicals postage paid at Duluth, MN 55806, and additional mailing offices. **POSTMASTER:** Please send address changes to **GPS WORLD**, P.O. Box 1270, Skokie, IL 60076-8270, USA. Canadian G.S.T. number: 840 033 278 RT0001, Publications Mail Agreement Number 40017597. Printed in the U.S.A.